MODELING OF PUNCHING SHEAR FAILURE OF LIGHTWEIGHT RC SLABS AND FERROCEMENT SLABS

Hany A. Dahish[1, 2] and Ahmed M. EL-Kholy[2]

[1]Civil Eng. Department, College of Engineering, Qassim University, Saudi Arabia.
E-mail: had00@fayoum.edu.eg
[2]Civil Eng. Department, Fayoum University, Fayoum, Egypt.
E-mail: amk00@fayoum.edu.eg

This paper presents numerical investigation for punching shear failure of normal and lightweight aggregate Reinforced Concrete (RC) slabs, and ferrocement slabs utilizing Expanded Metal Mesh (EMM) layer instead of regular flexural reinforcement. Three-dimensional nonlinear Finite Element Analysis (FEA) was applied to simulate the structural behavior and to estimate the punching shear strength of six concrete slabs. The modeled specimens involve slabs cast form normal weight RC, lightweight RC and cementitious mortar with reinforcement (grid of bars or layer of ferrocement) on the tension face. The concrete slabs were modeled using the finite element software ANSYS V.14. Both material and geometric nonlinearities were considered in modeling. Solid element and space bar were used to model the concrete and reinforcement grid, respectively. The EMM layer was considered as smeared layer embedded within the solid elements. The load-deflection behavior and crack pattern of the slabs were studied. The numerical results were validated with published experimental data, in terms of load capacity and maximum displacement. The numerical results appeared to be in good agreement with the experimental. The developed FE models provide good tool for predicting the punching shear resistance for RC slabs (normal and lightweight aggregate concrete), and cementitious slabs reinforced with mesh of bars or layer of ferrocement.

Keywords: Nonlinear FEA, normal and lightweight concrete slab, punching shear, ferrocement.

1 Introduction

The problem of punching shear is a major design concern and is considered a big issue in Reinforced Concrete (RC) slabs under concentrated loads or around columns because of the sudden and brittle failure. Many researchers investigated experimentally this issue for concrete slabs cast with different materials and reinforcements such as RC slabs cast with normal-weight or lightweight aggregate concrete (LWAC), and ferrocement slabs.

The use LWAC is not common due to its high cost. However, its high strength/weight ratio makes it a versatile construction material. Youm et al. (2013), conducted experimental program to study the punching shear behaviour of LWAC slabs with two different types of lightweight aggregates. Youm et al. (2013) concluded that the surface failure angle of punching shear is significantly affected by the type of utilized lightweight aggregate. Higashiyama et al. (2010) investigated a reduction factor for punching shear strength of five RC slabs cast with LWAC and revealed that the punching shear strength decreases with the density of LWAC.

Ferrocement is composite material that constructed by cement mortar with closely spaced layers of wire mesh for low-cost structural elements, Naaman (2000). Ferrocement can be used for water tanks and silos, and it needs no advanced techniques during installation. Ferrocement is the best alternative to concrete and steel as presented by Ibrahim (2011) who conducted 27 experimental tests on square cementitious slabs of 490x490x(40~60) mm simply supported on four edges and subjected to patch loading to investigate ultimate capacity of cementitious slabs with ferrocement layer or regular reinforcement grid. The test variables were the wire mesh volume fraction (0.12~1.41), slab thickness (40~60), and the patch load pattern (square or rectangular) and mesh type whether Welded Wire Mesh (WWM) or Expanded Metal Mesh (EMM). The test results showed that as the volume fraction increased the punching strength of the slabs was also increased and adding EMM mesh to ordinary reinforcement grid increases significantly the punching resistance at column stub. Mashrei (2012), developed a back-propagation neural network (BPNN) model to predict the punching shear strength of square ferrocement slabs based on data collected from different sources. Mansur et al. (2001), conducted 31 tests on simply supported square ferrocement slabs under central concentrated loading and concluded that the critical punching shear perimeter may be assumed at a distance equal to 1.5 times the slab thickness from the edge of the bearing plate. Paramasivam and Tan (1993) presented an experimental study to evaluate the punching shear strength of ferrocement slabs.

Being in the era of supercomputing, there is a tendency to replace the relatively expensive experimental investigations by numerical simulations. The use of large general purpose computer codes for the analysis of different types of aerospace, marine and civil engineering structures is by now well accepted. These programs have been used successfully to calculate the stress and deformation patterns of very complicated structural configurations with the accuracy demanded in engineering analysis. In the research presented in this paper, the punching shear failure of normal-weight RC slabs, LWAC RC slabs and cementitious slabs with ferrocement layers is numerically modeled using nonlinear finite element analysis (FEA). The numerical results were compared with published experimental results from Youm et al. (2013) and Ibrahim (2011) to validate the proposed finite element models. This research will be extended in a further paper to present intensive analysis for the influence of different parameters on the punching shear resistance of the considered concrete slabs types.

2 Details of Simulated Concrete Slabs

The developed FE models were based on the experimental plans of Youm et al. (2013) and Ibrahim (2011). Youm et al. (2013) experimental program consisted of testing one normal-weight concrete slab (NN) and two lightweight aggregate concrete slabs (LA and LD). All the three slabs had same dimensions and reinforcement layout. Figure 1a shows the dimensions of slabs and the layout of reinforcement. The cover depth is 20 mm for the top and the bottom reinforcements. The vertical displacement was applied through 300 mm square steel plates with thickness 35 mm.

Ibrahim (2011) experimental program consisted of testing 27 square cementitious slabs of 490x490x40~60 mm simply supported on four edges and subjected to patch loading. Three specimens (Slab-I, Slab-Ø6 and DP-2.0) were modeled in this paper. Slab-I was cast from plain mortar. Slab-Ø6 was a cementitious slab reinforced with 6mm steel bars arranged in two orthogonal directions and spaced 100 mm apart. DP-2.0 is a cementitious slab with ferrocement layer of EMM with strand thickness of 2 mm. The vertical displacement was applied through 80 mm square steel plate with thickness of 20 mm. The reinforcement layouts of Slab-Ø6 and DP-2.0 are shown in figures 1b and 1c, respectively.

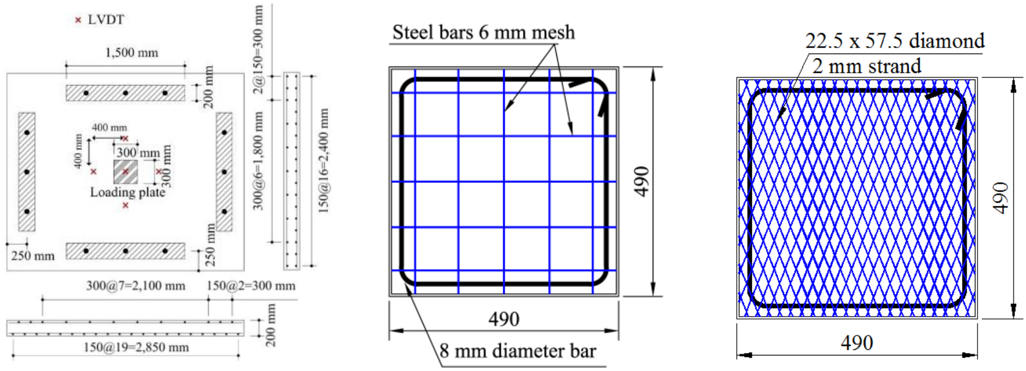

a. NN, LA and LD specimens (Youm et al., 2013)

b. Slab-Ø6 (Ibrahim, 2011)

c. DP-2.0 (Ibrahim, 2011)

Figure 1. Specimen dimensions and steel reinforcement details.

3 Finite Element Model

3.1 *Modeling concrete, ferrocement layer and reinforcement grid*

The slabs were simulated with ANSYS V.14 which offers robust nonlinear analysis capabilities. Routines were written in ANSYS to model the six specimens (NN, LA, LD, Slab-I, Slab-Ø6, DP-2.0) defined in section 2. The concrete element adopted in presented finite element model is Solid65. It is a three dimensional solid element (Figure 2) and has eight nodes with three degrees of freedom at each node (translations in x, y, and z directions). The element is capable of cracking in tension, crushing in compression, modeling the creep and simulating both material and geometrical nonlinearities. EMM layer was considered as smeared layer embedded within the solid elements. Two shear transfer coefficients, one for open cracks (0.3) and other for closed ones (0.6), were set to model the shear transfer in cracked concrete elements, Khan et al. (2014). Link8 element (Figure 3) was used to model the reinforcement grid for specimens without ferrocement layer. Link8 is a space bar element subjected to uniaxial force with three degrees of freedom (translations in x, y, and z directions) at each node. Link8 simulates material nonlinearity and large deformation behavior. Figure 4 shows the reinforcement bars model whereas figure 5 shows the meshing for the concrete solid elements.

3.2 *Material properties and plastic deformation*

Tables (1-4) and figures (6-7) illustrate the experimental data (Youm et al. 2013, Ibrahim 2011) which were used to develop presented numerical models. Table (1) lists the group classification, ID, compressive strength, tensile strength, modulus of elasticity and volume fraction for modeled slabs. Table (2) and figure 6 show the properties of Ø 10 mm bars used to reinforce group1 specimens. Table (3) defines the properties of Ø 6 mm bars used in Slab-Ø6 specimen. Table (4) lists the mechanical properties of EMM utilized in DP-2.0 specimen. Figure 7 shows the stress-strain curve for concrete f_c'=37.2 used to cast LA specimen. Poisson's ratios were set as 0.2 and 0.3 for concrete and steel, respectively.

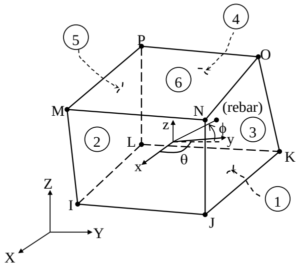

Figure 2. The geometry, node locations and coordinate system of Solid65 element

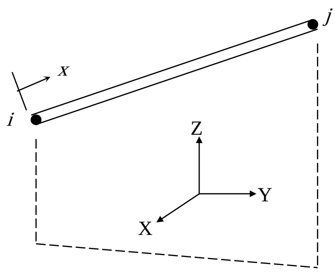

Figure 3. The geometry, node locations and coordinate system of Link8 element

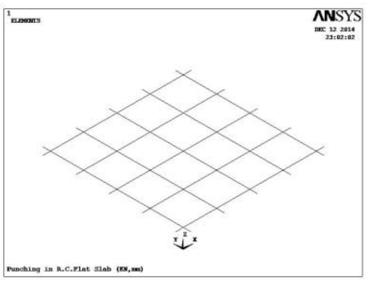

Figure 4. Meshed elements (link8) for modeling reinforcement grid

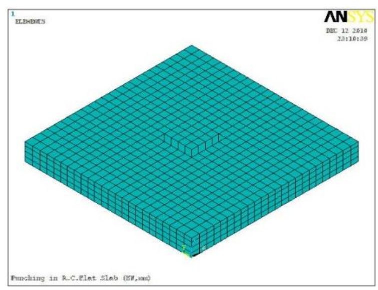

Figure 5. Meshed elements (solid65) for modeling concrete and cementitious slabs

Table 1. Material properties of modeled concrete and cementitous slabs

Group	Specimen	Thickness mm	Compressive strength f_c' (MPa)	Tensile strength f_{sp} (MPa)	Modulus of Elasticity E_c (GPa)	Volume fraction v_f	Reference
1	NN	200	40.6	3.41	31.7	---	Youm et al. (2013)
	LA	200	37.2	3.40	22.6	---	
	LD	200	34.2	2.82	20.0	---	
2	Slab-I	40	32.0	5.20	24.9	---	Ibrahim (2011)
	Slab-Ø6	50	32.0	5.20	24.9	1.41	
	DP-2.0	50	32.0	5.20	24.9	0.60	

Table 2. Properties of Ø10 mm steel bars

Yield stress	411 MPa
Ultimate strength	600 MPa
Elongation	12 %
Elastic modulus	200 GPa

Table 3. Properties of Ø6 mm steel bars

Yield stress	252 MPa
Ultimate strength	364 MPa
Elongation	30 %
Elastic modulus	195 GPa

Table 4. Mechanical properties of EMM

Diamond size	22.5x57.5 mm	Ultimate strength	500 MPa
Dimension of strand	2 mm	Ultimate strain	5.4%
Proof stress	300 MPa		
Proof strain	0.117%		

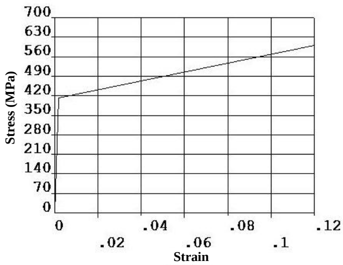

Figure 6. Stress-strain curve for steel bars 10 mm

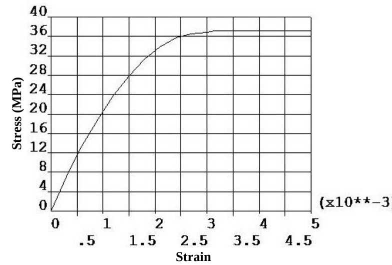

Figure 7. Stress-strain curve for utilized concrete (f_c' = 37.2 MPa)

3.3 *Loading and boundary conditions*

Displacement boundary conditions (restrained translations in x, y and z directions) were set at four edges of slabs to simulate the simply supported conditions similar to experiments. For top surface of loading plate, vertical displacement has been applied in fine increments in negative Z-direction for all joints to represent the actual loading procedure. Figures (8-9) show the boundary conditions at the four edges and the applied displacements for the two groups.

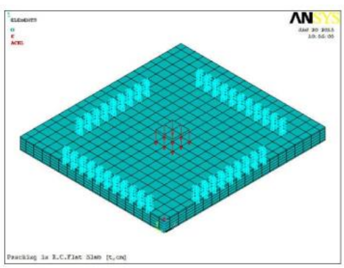

Figure 8. Restraints and applied displacements for first group

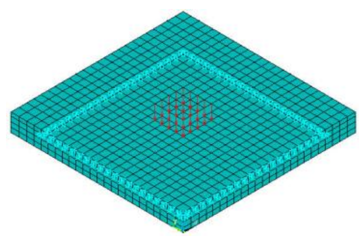

Figure 9. Restraints and applied displacements for second group

3.4 *Nonlinear analysis*

Because of non-linear nature of considered problem, the automatic time stepping is used to control the non-linear solution. The full Newton-Raphson method, Bathe (1996), was activated to solve the non-linear equations. Residual force convergence criterion has been applied with reasonable tolerance to control the convergence of the non-linear solution. The input data for nonlinear parameters of used materials has been provided in section (3.2).

3.5 *Bond behavior*

Bond between reinforcement bars and concrete was assumed perfect in accordance with that slab failure mode does not involve bond failure. Therefore, this assumption used in analysis will not cause a significant error in the predicted deformed shape and failure load.

4 Results

Table 4 and figures (10-11) show both numerical results and reference experimental results of ultimate load and deflection at slab center.

Table 4. Ultimate load and central deflection (numerical versus experimental)

Group	Specimen	Experimental results Youm et al. (2013) and Ibrahim (2011).		Numerical Results Proposed Model		Ratio Numerical/Experimental	
		Max. load (KN)	Deflection (mm)	Max. load (KN)	Deflection (mm)	Load	Deflection
1	NN	670.4	16.7	675.64	16.67	1.008	0.998
	LA	552.0	10.6	556.63	11.28	1.008	1.064
	LD	626.3	15.2	605.96	14.80	0.968	0.974
2	Slab-I	8.0	0.32	8.60	0.34	1.075	1.063
	Slab-Ø6	34.5	6.2	34.77	6.0	1.008	0.968
	DP-2.0	25.0	4.5	26.30	4.25	1.052	0.944

a. Group1

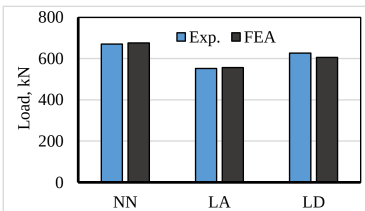

b.Group2

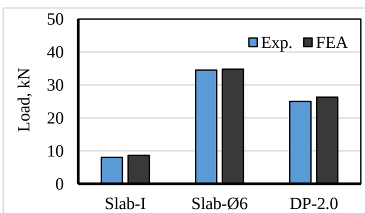

Figure 10. Ultimate load (FEA versus experiments)

a. Group1

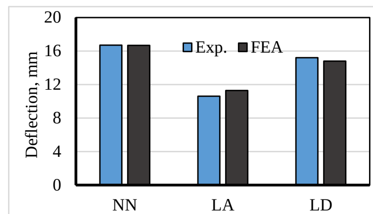

b.Group2

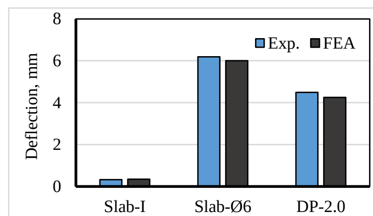

Figure 11. Central deflection (FEA versus experiments)

Figures (12-17) show the numerical and experimental load-deflection responses at centers of the considered six slabs. The numerical results show good agreement with experimental measurements. The variation between the numerical and experimental results was about 8% for failure loads and 7% for maximum deflections. Therefore, the proposed models give realistic estimations for failure loads and displacements. Figures (18-19) show comparisons between the numerical and experimental failure patterns, and deformed shapes for LA, LD and DP-2.0 slabs. The numerical results match well the experimental behavior.

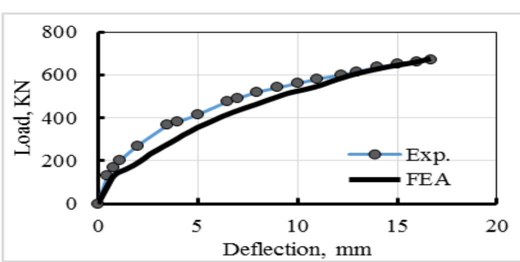

Figure 12. Load-Deflection response, NN slab

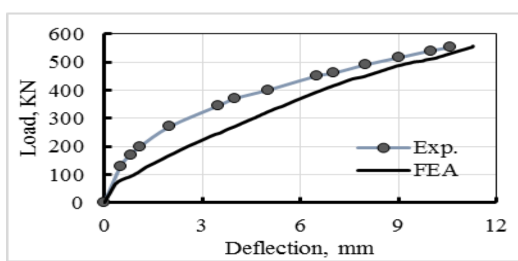

Figure 13. Load-Deflection response, LA slab

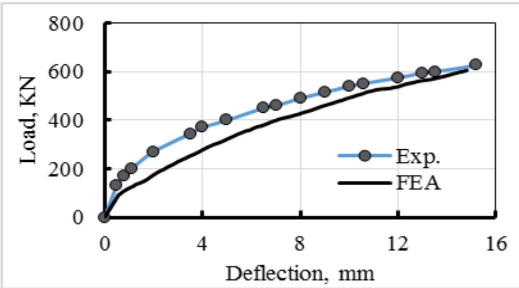

Figure 14. Load-Deflection response, LD slab

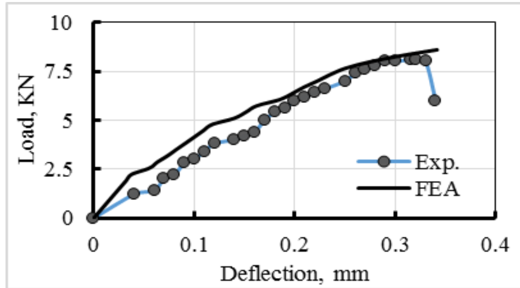

Figure 15. Load-Deflection response, Slab-I

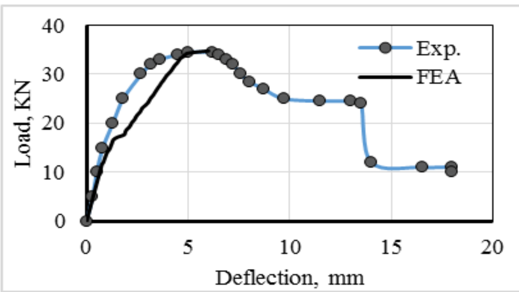

Figure 16. Load-Deflection response, Slab-Ø6

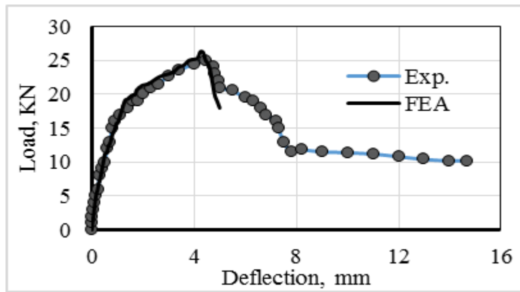

Figure 17. Load-Deflection response, DP-2.0 slab

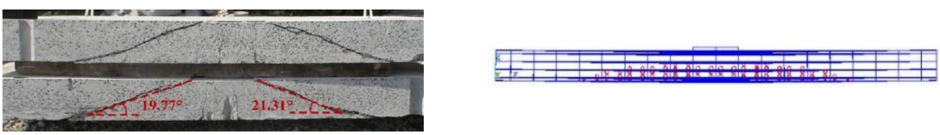

a. Experiment (Youm et al. 2013) b. Presented FEA

Figure 18. Failure Pattern for LA and LD slabs

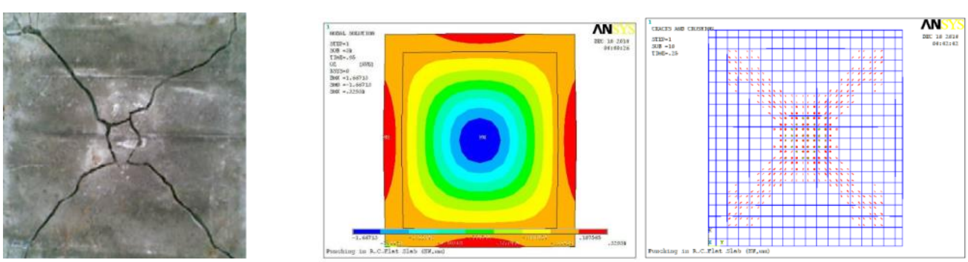

a. Experiment (Ibrahim 2011) b. Presented FEA

Figure 19. Deformed shape and failure pattern for DP-2.0 slab

5 Conclusions

In this paper, finite element modeling was presented by using ANSYS to predict the punching shear response and strength of different types of slabs: normal-weight RC slabs, lightweight aggregate RC slabs, cementitous slabs reinforced with regular grid of bars or with ferrocement layer and cementitious slabs without reinforcement. Three dimensional nonlinear FEA was conducted for six concrete slabs. The developed FE models were based on and compared with the experimental programs of Youm et al. (2013) and Ibrahim (2011). The predicted failure loads, maximum deflections, deformed shapes and failure patterns match well the experimental results. The non-linear finite element analysis is robust tool for analyzing the behavior of punching shear response of different types of cementitous and concrete slabs. The developed FE models could serve as a good tool for predicting the punching shear resistance for mentioned slabs types and save the high cost of experiments. Further exploring of the punching shear behavior and various parameters that affect the punching shear strength is now ready to be done numerically for large number of cases.

6 References

ANSYS (2009). *ANSYS User's Manual*. ANSYS, Inc., Southpointe, Canonsburg, PA, USA.

Bathe, K.J. (1996). *Finite Element Procedures*. Prentice-Hall, Inc.

Higashiyama, H., Mizukoshi, M. and Matsui, S. (2010). Punching shear strength of RC slabs using lightweight concrete. *Challenges, Opportunities and Solutions in Structural Engineering and Construction – Ghafoori (ed.)*. 111-117.

Ibrahim, H. M. (2011). Experimental investigation of ultimate capacity of wired mesh-reinforced cementitious slabs. *Constr Build Mater*, 25: 251-259.

Khan, H.U., Rafique, M.N., Karam, S., Ahmad, K. and Bashir A. (2014). Identification of shear cracks in reinforced beams using finite element method (ANSYS). *Pakistan J Sci*. 66(1): 50-55

Mansur, M.A., Ahmad, I., and Paramasivam, P. (2001). Punching shear strength of simply supported ferrocement slabs. *J. Mater. Civ. Eng –ASCE*. 13(6): 418-426.

Mashrei, M.A. (2012). Predicting punching shear strength of ferrocement slabs using back-propagation neural network. *Thi_Qar U J Eng Sci*. 3(2):85-102.

Naaman, A.E. (2000). *Ferrocement and laminated cementitious composites*. Techno Press 3000. Ann Arbor, Michigan, USA.

Paramasivam, P. and Tan, K. (1993). Punching shear strength of ferrocement slabs. *ACI Struct J*, 90(3): 294-301.

Youm, K.S., JEON, H.K., Park, Y.S., Lee, S.H. and Moon J. (2013). Experimental study on punching shear of lightweight concrete slab. *Proc. 13th East Asia-Pacific Conference on Structural Engineering and Construction (EASEC-13)*, September 11-13, 2013, Sapporo, Japan: easec13-E-6-4.